Journal of Alloys and Compounds 511 (2012) 232–236

Contents lists available at SciVerse ScienceDirect

Journal of Alloys and Compounds

journal homepage: www.elsevier.com/locate/jallcom

Nanocrystallization and photoluminescence of Ce/Dy/Eu-doped fluorosilicate glass ceramics

Xianping Fan [a], Xvsheng Qiao [a,*], Daliang Zhao [a], Qun Luo [a], Xianghua Zhang [b]

[a] State Key Laboratory of Silicon Materials, Department of Materials Science and Engineering, Zhejiang University, Hangzhou 310027, PR China
[b] UMR-CNRS 6512 "Verres & Ceramiques", Institut de Chimie de Rennes, Universite de Rennes 1 – Campus de Beaulieu, 35042 Rennes Cedex, France

ARTICLE INFO

Article history:
Received 6 July 2011
Received in revised form
14 September 2011
Accepted 15 September 2011
Available online 19 September 2011

Keywords:
Warm white light
Glass ceramics
Eu^{2+}
Ce^{3+}
Eu^{3+}

ABSTRACT

Ce^{3+}–Eu^{2+}–Dy^{3+}–Eu^{3+}-doped fluorosilicate glass ceramics containing orthorhombic $CaCeOF_3$ nanocrystals were prepared by annealing the precursor glass above 640 °C, along with the reduction of $Eu^{3+} \rightarrow Eu^{2+}$. Under near ultraviolet excitation, the emission bands of Eu^{2+} or Dy^{3+} were enhanced by several ten or hundred times, owing to energy transfers from Ce^{3+} to Eu^{2+} or Dy^{3+}. The glass and glass ceramics emitted warm white light deriving from the blue, yellow and red emission from Eu^{2+}, Dy^{3+} and Eu^{3+}. Tuning the annealing temperature, the Eu^{2+}/Eu^{3+} ratio and the warm white Commission Internationale de l'Eclairage (CIE) coordinates can be adjusted. Thus, the present materials can be applied on warm white high power light-emitting-diodes for indoor illumination application.

1. Introduction

White-light-emitting diodes (WLED) have been considered as new generation of illumination source, due to their tremendous advantages in energy use and related environmental benefits in comparison with the conventional incandescent and fluorescent lamps [1–3]. The market WLEDs are usually made up of blue-emitting InGaN–GaN LEDs and yellow-emitting YAG:Ce^{3+} phosphors [4–9] sealed with organic resins. But the poor heat-resistance and the relative low color rendering index (CRI) of such combination due to the lack of red emission baffle them to further apply on high power warm white LEDs for indoor illumination [10,11]. In order to overcome these problems, it was essential to develop luminescent materials that emitted directly white light containing all color components, especially red components. Although the phosphors have been widely investigated for this purpose [12,13], the glass-ceramics might be a good alternatives for WLEDs, due to its better heat-resistance, easy of formability, and low porosity compared with sintered ceramics [14–22].

In this paper, luminescence properties of Ce^{3+}, Eu^{2+}, Dy^{3+} and Eu^{3+} single-doped and tetra-doped fluorosilicate glass and glass ceramics are investigated. Ce^{3+} and Eu^{2+} are characterized by their f–d transitions, exhibiting large absorption band and intense emission intensity, so widely utilized as phosphor dopants [23–26]. In the present fluorosilicate host, Ce^{3+} has extremely larger absorption cross section than Eu^{2+}, but its emission band locates at ultraviolet region, unlike that of Eu^{2+} in visible region. Therefore, we select Ce^{3+} as sensitizers and Eu^{2+} as activators to produce intense broad visible emission band. Besides, the emission bands of Dy^{3+} might play an important role in the white light emission adjusting, which can be enhanced greatly by energy transfer (ET) from Ce^{3+} to Dy^{3+}. And the red emission of Eu^{3+} provides good makeup to CRI.

2. Experimental

The glasses were prepared according to the compositions listed in Table 1 with the weight accuracy of 0.001 g, where GCe, GDy, GEu and GCEu are reference samples for GCeDyEu. Glass components were introduced with high purity SiO_2, Al_2O_3, CaF_2, CeF_3, DyF_3 and EuF_3 raw materials. The well mixed raw materials were put in a corundum crucible and placed into a muffle furnace, where the corundum crucible was covered with a large graphite crucible to produce reduction atmosphere at high temperatures. They were melted at 1350 °C for 35 min. The melt was poured on a brass mould and pressed by another brass plate to obtain glass samples. Subsequently, glass ceramics were obtained by annealing GCeDyEu and GEu in the air according to the methods listed in Table 1. All the glass and glass ceramics were polished on a UNIPOL-802 precision lapping/polishing machine to get optical quality for optical measurements.

Differential Thermal Analyzer (DTA) measurements for glass samples were carried out on a CDR-1 Differential Thermal Analyzer in the air with a heating rate of 10 °C/min to determine the glass transition temperature (T_g) and the crystallized peak temperature (T_c). Powder X-ray diffraction (XRD) measurements were performed on a XD-98 diffractometer with Common Bragg Diffraction Continuous Scanning Mode, Cu-K_α radiation at 4°/min scanning rate and 0.02° step size. From XRD patterns, crystal sizes, d-spacing and their random errors were evaluated using

* Corresponding author. Tel.: +86 571 87952334; fax: +86 571 87951234.
E-mail address: qiaoxus@zju.edu.cn (X. Qiao).

0925-8388/$ – see front matter © 2011 Elsevier B.V. All rights reserved.
doi:10.1016/j.jallcom.2011.09.042

Table 1
Compositions of the glass samples, and annealing methods of the glass ceramic samples.

Glass	Composition (mol%)	Glass ceramics	Annealing methods
GCeDyEu	$50SiO_2$–$20Al_2O_3$–$20CaF_2$ –$8CeF_3$–$1DyF_3$–$1EuF_3$	GC640	GCeDyEu, 4 h @ 640
		GC660	GCeDyEu, 4 h @ 660
GCe	$50SiO_2$–$20Al_2O_3$–$20CaF_2$–$10CeF_3$	GC680	GCeDyEu, 4 h @ 680
GDy	$50SiO_2$–$20Al_2O_3$–$20CaF_2$–$10DyF_3$	GC780	GCeDyEu, 4 h @ 780
GEu	$50SiO_2$–$20Al_2O_3$–$27CaF_2$–$3EuF_3$	GCEu	GEu, 12 h @ 680

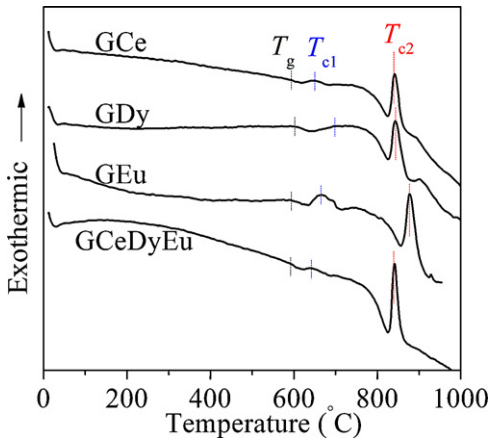

Fig. 1. DTA curves of GCe, GDy, GEu and GCeDyEu.

Jade (Materials Data, Inc.). The steady photoluminescence (PL) measurements were performed on a Hitachi F-4500 fluorescence spectrophotometer. The time resolved spectra were measured with an Edinburgh FLS920P spectrometer using excitation from a EPL405 picosecond LD pulsed laser, a nF900 nanosecond hydrogen flash lamp or a μF900 microsecond flash lamp. All spectroscopic measurements were performed at room temperature. Systematical errors in the above measurements were minimized by calibrating instruments with standard samples.

3. Results and discussion

Fig. 1 shows DTA curves of GCe, GDy, GEu and GCeDyEu. Accordingly, the glass transition temperatures (T_g) and crystallization peak temperatures (T_c) of the glass samples can be determined. The glass samples have similar T_g at the range of 590–600 °C, but different glass presents different T_c. GCe, GDy, GEu and GCeDyEu show the first crystallization peaks (T_{c1}) respectively at 650 °C, 698 °C, 665 °C and 642 °C, and the second crystallization peaks (T_{c2}) respectively at 839 °C, 844 °C, 877 °C and 839 °C. GEu presents its T_{c2} at higher temperature (877 °C) than those of the other glasses (around 840 °C), which is related with the lower rare earth content of GEu (3 mol%) than those of the other (10 mol due to rare earth ions here may be nucleating agents. According to the heat treatment of the glasses around T_c and the subsequent XRD analysis, T_{c1} corresponds to the precipitation of fluoride or oxyfluoride phases, and T_{c2} corresponds to the crystallization process of the whole glass components (the whole crystallization fraction can be up to 100%). Such fluoride phase at T_{c1} is orthorhombic $CaCeOF_3$ for GCe and GCeDyEu, and is cubic CaF_2 for GDy and GEu. Accordingly, we annealed GCeDyEu at 640 °C, 660 °C, 680 °C and 780 °C to get glass ceramic samples containing $CaCeOF_3$ crystalline phase.

Fig. 2 shows XRD patterns of GCeDyEu and the glass ceramics obtained by annealing GCeDyEu at different temperatures. XRD patterns of the glass ceramic samples appear sharp diffraction peaks on the broad glassy diffraction base, while that of glass sample shows completely amorphous exhibiting no diffraction peaks. The diffraction peaks of GC640, GC660 and GC680 are easily assigned to orthorhombic $CaCeOF_3$ (PDF# 21-0136), but those of GC780 are assigned to hexagonal $CaCeF_6$ (major phase, PDF# 21-0135) and cubic $Ce_3O_4F_3$ (minor phase, PDF# 21-0184). From the

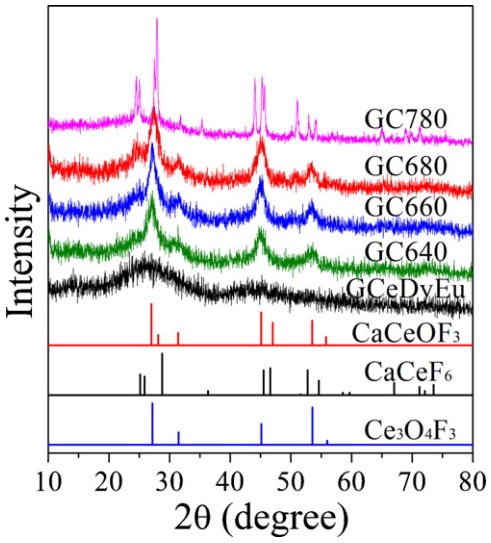

Fig. 2. XRD patterns of GCeDyEu and the glass ceramics obtained by annealing GCeDyEu at different temperatures, and standard PDF card of orthorhombic $CaCeOF_3$ (PDF# 21-0136), hexagonal $CaCeF_6$ (PDF# 21-0135) and cubic $Ce_3O_4F_3$ (PDF# 21-0184).

broadening of diffraction peaks, crystal size can be evaluated by the Scherrer formula, and the volume fraction of the crystalline phase (crystallinity) can be estimated by the ratio of the integrated area of the diffraction peaks to the total area of the XRD pattern from 10° to 80°. The calculated results are list in Table 2. With the annealing temperature increasing from 640 °C to 680 °C, the crystal size and the crystallinity of the precipitated $Ce_3O_4F_3$ show slow increasing tendencies, from (6.0 nm, 34.66%) to (7.3 nm, 42.33%). The $CaCeOF_3$ nanophase are so small in size that GC640, GC660 and GC680 keep high transparency in visible to near infrared range. When the annealing temperature is up to 780 °C, the crystalline phase shifts to $CaCeF_6 + Ce_3O_4F_3$ with sizes larger than 39 nm and a whole crystallinity of about 43%. It leads GC780 to loss its transparency. Obviously, such crystal phase shift from $CaCeOF_3$ to $CaCeF_6 + Ce_3O_4F_3$ goes with the transfer of $Ce^{3+} \rightarrow Ce^{4+}$. It is

Table 2
Crystalline phase in the glass ceramic samples and their crystal sizes and crystallinity evaluated from XRD data.

Glass ceramics	Crystalline phase	Crystal size (nm)	Crystallinity (%)
GC640	Orthorhombic $CaCeOF_3$	6.0 ± 0.2	34.66 ± 1.78
GC660	Orthorhombic $CaCeOF_3$	6.9 ± 0.2	39.04 ± 2.47
GC680	Orthorhombic $CaCeOF_3$	7.3 ± 0.2	42.33 ± 2.83
GC780	Hexagonal $CaCeF_6$ Cubic $Ce_3O_4F_3$	39.0 ± 0.5 45.8 ± 0.8	27.35 ± 1.05 15.70 ± 0.55

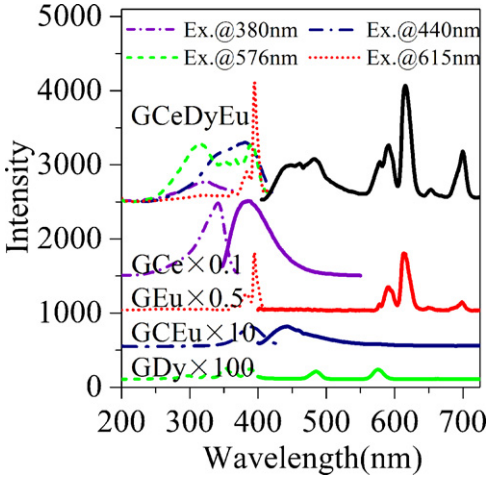

Fig. 3. Excitation and emission spectra of GCeDyEu, GCe, GEu, GCEu and GDy. Excitation spectra were record with monitoring at 380 nm (for Ce^{3+}), 440 nm (for Eu^{2+}), 576 nm (for Dy^{3+}) and 615 nm (for Eu^{3+}) and exciting at 395 nm. Emission spectra were record with exciting at 340 nm (for GCe), 380 nm (for GCEu), 380 nm (for GDy) and 395 nm (for GEu and GCeDyEu).

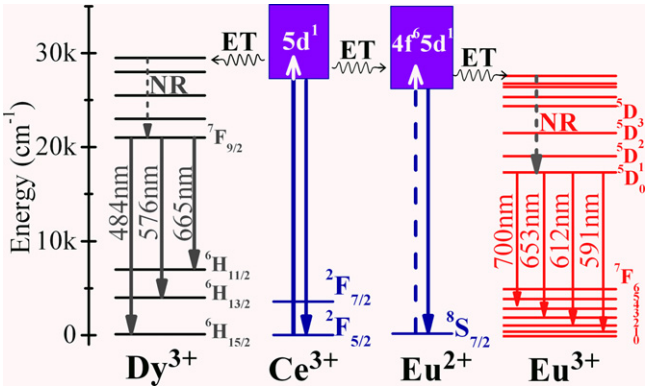

Fig. 4. Simplified energy level diagrams of Dy^{3+}, Ce^{3+}, Eu^{2+} and Eu^{3+}, and possible energy transfers (ET) among Dy^{3+}, Ce^{3+}, Eu^{2+} and Eu^{3+} in the investigated glass and glass ceramics.

probably owing to the direct oxidation by oxygen in the air and the charge compensation to $Eu^{3+} \rightarrow Eu^{2+}$. The Eu^{3+} ions are easily reduced to Eu^{2+} ions during the annealing processes, which could be confirmed by the XRD peak shift. According to Bragg diffraction formula, one can find interplanar spacings of $CaCeOF_3$ and $CaCeF_6$ in the glass ceramics are larger than those of the standard PDF card. That may be attributed to Eu^{3+} substituting Ca^{2+} during the annealing process and the simultaneous reduction of $Eu^{3+} \rightarrow Eu^{2+}$ in order to keep charge balance of the Eu_{Ca} site. Because Eu^{2+} has lager ionic radius (0.125 nm) than Ca^{2+} (0.108 nm), the interplanar spacings of $CaCeF_6$:Eu^{2+} become smaller than those of the standard. For Dy^{3+} ions, they also easily substitute Ca^{2+} or Ce^{3+} and enter the precipitated nanocrystals, since Dy^{3+} has the smaller ionic radius (0.099 nm) with Ca^{2+} (0.108 nm) and Ce^{3+} (0.109).

To explain the reduction phenomenon of $Eu^{3+} \rightarrow Eu^{2+}$, the substitution defect model or charge compensation modern has been proposed [27,28]. When trivalent Eu^{3+} ions were doped into those hosts containing M^{2+} (M = Ca^{2+}, Sr^{2+}, Ba^{2+} and Zn^{2+}), Eu^{3+} would replace the M^{2+} ions. In order to keep the charge balance of the M^{2+} site, Eu^{3+} ions were reduced to Eu^{2+} ions. In the present case, the oxidation of $Ce^{3+} \rightarrow Ce^{4+}$ happens to compensate the whole charge balance. So the process could be described as the following:

$$Ca_{Ca} + Eu^{3+} + Ce^{3+} \rightarrow Eu_{Ca} + Ca^{2+} + Ce^{4+} \quad (1)$$

Other literatures [29] also reported the Eu^{3+}–Ce^{3+} pairs easily transfer to the stable Eu^{2+}–Ce^{4+} pairs. Similarly, GCEu contains CaF_2:Eu^{2+} nanocrystals other than CaF_2:Eu^{3+} due to the reduction of Eu^{3+} substituting Ca^{2+} during the annealing process and the simultaneous reduction of $Eu^{3+} \rightarrow Eu^{2+}$. And these can be confirmed by the following PL spectra.

Fig. 3 shows the excitation and emission PL spectra of GCeDyEu, GCe, GEu, GCEu, and GDy. GCe has broad excitation and emission bands respectively centered at 340 nm and 380 nm, which are assigned to 4f→5d transitions of Ce^{3+} ions. Similarly, GCEu also has broad excitation and emission bands respectively centered at 380 nm and 440 nm, which are assigned to 4f→5d transitions of Eu^{2+} ions. However, GEu and GDy only present luminescence of 4f→4f transitions. The excitation bands of GDy are assigned to the $^6H_{15/2} \rightarrow {}^6P_{3/2}$ (324 nm), $^6H_{15/2} \rightarrow {}^6P_{7/2}$ (350 nm), $^6H_{15/2} \rightarrow {}^4P_{3/2}$ (364 nm) and $^6H_{15/2} \rightarrow {}^4F_{7/2}$ (386 nm) transitions of Dy^{3+} ions, and the emission spectrum GDy consisted of the emission peaks corresponding to $^4F_{9/2} \rightarrow {}^6H_{15/2}$ (484 nm) and $^4F_{9/2} \rightarrow {}^6H_{13/2}$ (576 nm) transitions of Dy^{3+} ions. The excitation bands of GEu are assigned to the transitions of $^7F_0 \rightarrow {}^5D_4$ (363 nm), $^7F_0 \rightarrow {}^5G_{2,3,4,5,6}$ (383 nm), $^7F_0 \rightarrow {}^5L_6$ (395 nm) excitation bands of Eu^{3+}, and the emission spectrum of GEu consisted of the emission peaks corresponding to $^5D_0 \rightarrow {}^7F_0$ (578 nm), $^5D_0 \rightarrow {}^7F_1$ (591 nm), $^5D_0 \rightarrow {}^7F_2$ (615 nm), $^5D_0 \rightarrow {}^7F_3$ (650 nm) and $^5D_0 \rightarrow {}^7F_4$ (700 nm) transitions of Eu^{3+} ions. By comparison, in the present glass host, the excitation band of Ce^{3+} is found to be several tens or hundreds times stronger than that of Eu^{2+} or Dy^{3+}, and their excitation bands partially overlapped to each other. According to energy transfer theory [30], Ce^{3+} ions can be sensitizers for Eu^{2+} or Dy^{3+} and enhance the emission intensity of Eu^{2+} or Dy^{3+} efficiently. Similarly, Eu^{2+} ions can be sensitizers for Dy^{3+} or Eu^{3+}. But the excitation intensity or absorption cross section of Eu^{2+} is much weaker than that of Ce^{3+}, the enhancement effect by ETs from Eu^{2+} to Dy^{3+} or Eu^{3+} is not as efficient as Ce^{3+}. The above possible energy transfers are illustrated in Fig. 4.

With reference to the spectra of the single doped samples in Fig. 3, one can find the emission spectrum of GCeDyEu is composed with the parts deriving from Eu^{2+}, Dy^{3+} and Eu^{3+}. The excitation bands corresponding to Eu^{2+} (monitoring at 440 nm) or Dy^{3+} (monitoring at 576 nm) is significantly enhanced in GCeDyEu than those in GCEu and GDy, while excitation bands of Ce^{3+} in GCeDyEu is several ten times weaker than that in GCeDyEu than that in GCe. It indicates that the above mentioned ET from Ce^{3+} to Eu^{3+} or Dy^{3+} is reasonable in the present glass system. There is no obvious difference between the Eu^{3+} luminescence of GCeDyEu and GEu. It suggests no efficient ET between Ce^{3+} and Eu^{3+}. But here Eu^{3+} indeed acts as an important red luminescence activator to get warm white light. According to 1931 CIE-XYZ Coordinate System [31] of the Commission Internationale de l'Eclairage (CIE), CIE coordinate of GCeDyEu is calculated as (0.38, 0.27), which yields the warm white light. Thus, the present $50SiO_2$–$20Al_2O_3$–$22CaF_2$–$8CeF_3$–$1DyF_3$–$1EuF_3$ glass can be considered as potential warm white light phosphors applying on indoor high power LED.

In order to improve the luminescence of GCeDyEu, we annealed it at different temperatures above its T_{c1}, and got a series of glass ceramics named as GC640, GC660, GC680 and GC780. Fig. 5 shows the emission spectra of such glass ceramics. With the annealing temperature increasing, blue emission deriving from Eu^{2+} and Dy^{3+} is strengthened, while red emission deriving from Eu^{3+} is weakened. This suggests the enrichment of Eu^{3+} and Dy^{3+} into the precipitated nanocrystals and the reduction of $Eu^{3+} \rightarrow Eu^{2+}$ took place along with the annealing process of the glass ceramics. For GC640, GC660 and GC680, only a part of Eu^{3+} convert to Eu^{2+}, so these samples present blue and red emission simultaneously. For GC780, almost all of Eu^{3+} ions convert to Eu^{2+} ions, so GC780 only

Table 3
The lifetimes of the luminescence of Ce^{3+}, Eu^{2+}, Dy^{3+} and Eu^{3+} in the investigated samples determined from luminescence decay curves.

Sample name	τ (ns) Ce^{3+} @ 360 nm	τ (μs) Eu^{2+} @ 440 nm	τ (ms) Dy^{3+} @ 576 nm	τ (ms) Eu^{3+} @ 615 nm
GCe	35.9			
GCEu		0.667		
GDy			0.742	
GEu				2.53
GCeDyEu	13.9	0.496	0.860	1.90
GC640	11.9	0.539	0.871	1.89
GC660	11.7	0.412	0.754	1.92
GC680	9.3	0.321	0.641	2.59
GC780		0.092		

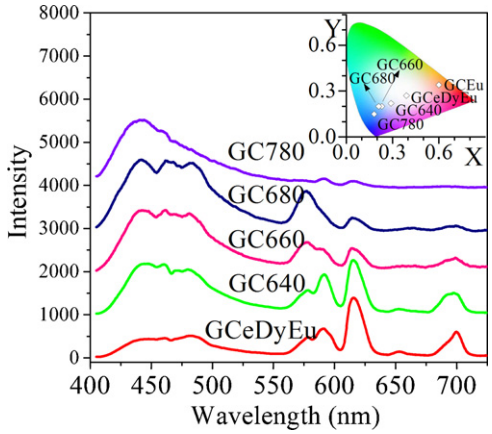

Fig. 5. Emission spectra of GCeDyEu and the glass ceramics obtained by annealing GCeDyEu at different temperatures with exciting at 395 nm. The inset graph shows CIE (*X*,*Y*) color coordinate diagram of the samples.

has blue emission band of Eu^{2+}. But GC780 presents no intense emission of Dy^{3+}, which suggests no efficient ET from Eu^{2+} to Dy^{3+} in the present system. So we believe ET from Ce^{3+} to Eu^{2+} or Dy^{3+} is major and efficient, and ET from Eu^{2+} to Dy^{3+} or Eu^{3+} is less efficient. As shown in the inset graph of Fig. 5, from GCEu to GCeDyEu to GC780, the luminescence color appear a change from red to warm white to blue. Accordingly, one can tune the ratio of Eu^{2+}/Eu^{3+} and the luminescence color coordinate by annealing methods.

By monitoring the luminescence of Ce^{3+} at 360 nm, Eu^{2+} at 440 nm, Dy^{3+} at 576 nm and Eu^{3+} at 615 nm, we obtained the luminescence decay curves of the investigated glass and glass ceramics, as Fig. 6 shows. All the luminescence decays of Dy^{3+} and Eu^{3+} yield nearly single exponential laws, while those of Ce^{3+} and Eu^{2+} are non-exponential except in GCe and GCEu. It is probably led by the introduction of extra decay pathways due to the ETs from Ce^{3+}/Eu^{2+}

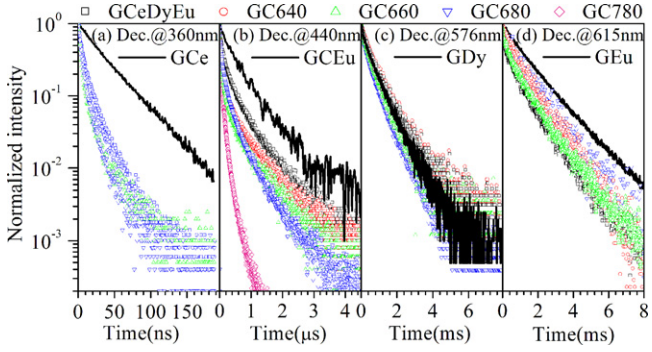

Fig. 6. Luminescence decay curves of the investigated glass and glass ceramics by monitoring the luminescence of Ce^{3+} at 360 nm, Eu^{2+} at 440 nm, Dy^{3+} at 576 nm and Eu^{3+} at 615 nm, respectively. (The vertical axis is logarithmic.)

to other rare earth ions in the samples. Using the following formula, the average luminescence lifetime can be evaluated:

$$\tau = \frac{\int_0^\infty I(t)\cdot t\ dt}{\int_0^\infty I(t)\,dt} \quad (2)$$

where $I(t)$ is the luminescence intensity at the time t. The calculated lifetime of Ce^{3+}, Eu^{2+}, Dy^{3+} and Eu^{3+} in the glass and glass ceramics are listed in Table 3. The luminescence decays of Ce^{3+} in the codoped samples are much faster than that in GCe. The faster decline could be explained by the introduction of extra decay pathways due to the Dy/Eu-doping. ET from Ce^{3+} to Eu^{2+} or Dy^{3+} enhanced the decay rate of the excited Ce^{3+}. According to the energy transfer theory [30], the ET rate has the following relationship with the distances between the sensitizer and activator ions (r_{D-A}):

$$W_{ET} \propto \frac{1}{r_{D-A}^6} \quad (3)$$

For the glass ceramics annealed around T_{c1}, the ET processes can be strengthened by the much closer inter-ionic distance due to the enrichment of Eu^{2+} and Dy^{3+} into the precipitated $CaCeOF_3$. Resultantly, the PL lifetime of Ce^{3+} in the glass ceramics appear a decreasing tendency with the annealing temperature increasing. At the same time, with the annealing temperature increasing, Eu^{2+} become more while Eu^{3+} become less due to the reduction of $Eu^{3+} \rightarrow Eu^{2+}$ mentioned before. Because of the so-called "luminescence concentration quenching" effect, the PL lifetime of Eu^{2+} in the glass ceramics decrease significantly along with the annealing temperature increasing. The PL lifetime of Eu^{3+} presents a converse varying tendency due to the reduction of Eu^{3+}. The PL lifetime of Dy^{3+} in the glass ceramics also become short along with the annealing temperature increasing, due to the local enrichment of Dy^{3+} in the precipitated $CaCeOF_3$.

4. Conclusions

We prepared Ce^{3+}–Dy^{3+}–Eu^{2+}–Eu^{3+}-codoped fluorosilicate glass under reducing atmosphere. By annealing the precursor glass around 640 °C, orthorhombic $CaCeOF_3$ nanocrystalline phase precipitated in the glass matrix. The reduction of $Eu^{3+} \rightarrow Eu^{2+}$ took place along with the annealing process, owing to Eu^{3+} substituting Ca^{2+} sites in $CaCeOF_3$. The Eu^{2+}/Eu^{3+} ratio can be fine adjusted by tuning the annealing temperature within the first crystallization peak covering region. The ET from Ce^{3+} to Eu^{2+} or Dy^{3+} is major and efficient, while those from Eu^{2+} to Dy^{3+} or Eu^{3+} is less efficient. Combining emission bands of Eu^{2+}, Dy^{3+} and Eu^{3+}, the glass and glass ceramics emit warm white light with tunable CIE coordination. Thus, the Eu/Dy doped SiO_2–Al_2O_3–CaF_2 –CeF_3 glass and glass ceramics can be demonstrated to be a potential warm white light emitting materials applied on high power LED for future indoor illumination.

Acknowledgements

This work is supported by the National Nature Science Foundation of China (No. 50902120), the Research Fund of the Doctoral Program of Higher Education of China (No. 20100101120025), Science and Technology Innovative Research Team of Zhejiang Province (No. 2009 R50010), China–France Cooperative Program Cai Yuanpei 2010–2012 and Program for Changjiang Scholars and Innovative Research Team in University.

References

[1] M.R. Krames, O.B. Shchekin, R. Mueller-Mach, G.O. Mueller, Z. Ling, G. Harbers, M.G. Craford, J. Disp. Technol. 3 (2007) 160–175.
[2] E.F. Schubert, J.K. Kim, Science 308 (2005) 1274–1278.
[3] M.P. Saradhi, U.V. Varadaraju, Chem. Mater. 18 (2006) 5267–5272.
[4] J.K. Park, M.A. Lim, C.H. Kim, H.D. Park, J.T. Park, S.Y. Choi, Appl. Phys. Lett. 82 (2003) 683–685.
[5] R.J. Xie, N. Hirosaki, M. Mitomo, K. Takahashi, K. Sakuma, Appl. Phys. Lett. 88 (2006) 101104.
[6] C.F. Guo, Y. Xu, X. Ding, M. Li, J. Yu, Z.Y. Ren, J.T. Bai, J. Alloys Compd. 509 (2011) L38–L41.
[7] H. He, X.F. Song, R.L. Fu, Z.W. Pan, X.R. Zhao, Z.H. Deng, Y.G. Cao, J. Alloys Compd. 493 (2010) 401–405.
[8] C.F. Guo, Y. Xu, F. Lv, X. Ding, J. Alloys Compd. 497 (2010) L21–L24.
[9] I.M. Nagpure, K.N. Shinde, S.J. Dhoble, A. Kumar, J. Alloys Compd. 481 (2009) 632–638.
[10] A. Engel, M. Letz, T. Zachau, E. Pawlowski, K. Seneschal-Merz, T. Korb, D. Enseling, B. Hoppe, U. Peuchert, J.S. Hayden, Proc. SPIE 6486 (2007), 64860Y.1–64860Y.10.
[11] J.S. Kim, P.E. Jeon, J.C. Choi, H.L. Park, S.I. Mho, G.C. Kim, Appl. Phys. Lett. 84 (2004) 2931–2933.
[12] W.J. Yang, T.M. Chen, Appl. Phys. Lett. 88 (2006) 101903.
[13] S.H. Lee, J.H. Park, S.M. Son, J.S. Kim, H.L. Park, Appl. Phys. Lett. 89 (2006) 221916.
[14] G.J. Gao, N. Da, S. Reibstein, L. Wondraczek, Opt. Express 18 (2010) A575–A583.
[15] Z. Cui, R. Ye, D. Deng, Y. Hua, S. Zhao, G. Jia, C. Li, S. Xu, J. Alloys Compd. 509 (2011) 3553–3558.
[16] R. Ye, Z. Cui, Y. Hua, D. Deng, S. Zhao, C. Li, S. Xu, J. Non-Cryst. Solids 357 (2011) 2282–2285.
[17] S. Taruta, M. Matsuki, H. Nishikiori, T. Yamakami, T. Yamaguchi, K. Kitajima, Ceram. Int. 36 (2010) 1303–1309.
[18] Z. Cui, R. Ye, Y. Hua, D. Deng, S. Zhao, C. Li, S. Xu, J. Non-Cryst. Solids 357 (2011) 2298–2301.
[19] Z. Cui, G. Jia, D. Deng, Y. Hua, S. Zhao, L. Huang, H. Wang, H. Ma, S. Xu, J. Lumin. 132 (2012) 153–160.
[20] L.Y. Xiao, Q. Xiao, Y.L. Liu, P.F. Ai, Y.D. Li, H.J. Wang, J. Alloys Compd. 495 (2010) 72–75.
[21] Q. Luo, X.S. Qiao, X.P. Fan, X.H. Zhang, J. Non-Cryst. Solids 356 (2010) 2875–2879.
[22] D.Q. Chen, Y.L. Yu, P. Huang, H. Lin, Z.F. Shan, Y.S. Wang, Acta Mater. 58 (2010) 3035–3041.
[23] J.S. Kim, P.E. Jeon, Y.H. Park, J.C. Choi, H.L. Park, Appl. Phys. Lett. 85 (2004) 3696–3698.
[24] R.J. Yu, J. Wang, J.H. Zhang, H.B. Yuan, Q. Su, J. Solid State Chem. 181 (2008) 658–663.
[25] G. Blasse, A. Bril, J. Chem. Phys. 47 (1967) 5139–5145.
[26] D.H. Gahane, N.S. Kokode, P.L. Muthal, S.M. Dhopte, S.V. Moharil, J. Alloys Compd. 484 (2009) 660–664.
[27] Z. Lian, J. Wang, Y.H. Lv, S.B. Wang, Q. Su, J. Alloys Compd. 430 (2007) 257–261.
[28] M.Y. Peng, Z.W. Pei, G.Y. Hong, Q. Su, Chem. Phys. Lett. 371 (2003) 1–6.
[29] G. Blasse, A. Bril, J. Chem. Phys. 47 (6) (1967) 1920–1926.
[30] D.L. Dexter, J. Chem. Phys. 21 (1953) 836–850.
[31] M. Shaw, M. Fairchild, Color Res. Appl. 27 (5) (2002) 316–329.